Published in final edited form as:
Anal Chem. 2018 April 17; 90(8): 5239–5246. doi:10.1021/acs.analchem.8b00012.

Shotgun Analysis of Diacylglycerols Enabled by Thiol–ene Click Chemistry

Sarju Adhikari[†,‡], **Wenpeng Zhang**[†,‡], **Xiaobo Xie**[†], **Qinhua Chen**[§], and **Yu Xia**[*,†,‡]

[†]Department of Chemistry, MOE Key Laboratory of Bioorganic Phosphorus Chemistry & Chemical Biology, Tsinghua University, Beijing 100084, China

[‡]Department of Chemistry, Purdue University, West Lafayette, Indiana 47906, United States of America

[§]Affiliated Dongfeng Hospital, Hubei University of Medicine, Shiyan, Hubei Province 442000, China

Abstract

Diacylglycerols (DAGs) are a subclass of neutral lipids actively involved in cell signaling and metabolism. Alteration in DAG metabolism has been associated with onset and progression of several human-related diseases. The structural diversity of DAGs and their low concentrations in biological samples call for the development of methods that are capable of sensitive identification and quantitation of each DAG species as well as rapid profiling when a biochemical pathway is perturbed. In this work, the thiol–ene click chemistry has been employed to introduce a charge-tag, namely, cysteamine (CA), at a carbon–carbon double bond (C=C) of unsaturated DAGs. This one-pot photochemical derivatization is fast (within 1 min), universal (monotagging) for DAGs varying in fatty acyl chain lengths and the number of C=Cs, and suitable for small sample volume (e.g., 1–50 μL plasma). Because of the presence of the amine group in CA, tagged DAGs showed at least 10 times increase in response to electrospray ionization as compared to conventional ammonium adduct formation. Low-energy collision-induced dissociation of CA tagged DAGs allowed confident assignment of fatty acyl composition. A neutral loss scan based on characteristic 95 Da loss (a combined loss of CA and H_2O) of tagged DAGs has been established as a sensitive means for unsaturated DAG detection (limit of detection = 100 pM) and quantitation from mixtures. The analytical utility of CA tagging was demonstrated by shotgun analysis of unsaturated DAGs in human plasma, including samples from type 2 diabetes mellitus patients.

[*]**Corresponding Author:** xiayu@mail.tsinghua.edu.cn.

Supporting Information

The Supporting Information is available free of charge on the ACS Publications website at DOI: 10.1021/acs.anal-chem.8b00012. Additional information on extraction protocols for DAGs from human plasma, optimization of experimental parameters, and MS data on analysis of DAGs from human plasma (PDF)

ORCID
Yu Xia: 0000-0001-8694-9900

Author Contributions

All authors have given approval to the final version of the manuscript.

Notes

The authors declare no competing financial interest.

Graphical abstract

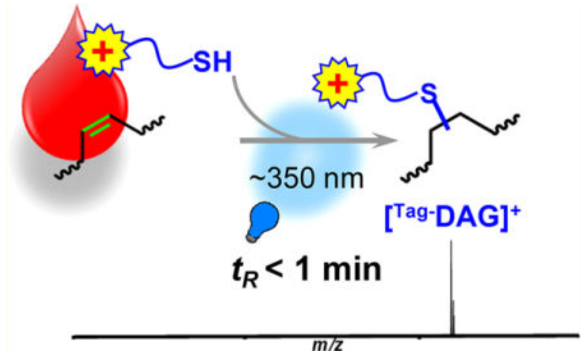

Neutral lipids, including sterol lipids and glycerol lipids, are important components of cellular lipidomes, performing distinct biological functions as compared to polar lipids. As a subclass of glycerol lipids, diacylglycerols (DAGs) share a generic structure, in which two hydroxyl groups in the glycerol backbone are substituted by fatty acyls through ester bonds. DAGs play a variety of roles inside cells; they are produced as metabolites of triacylglycerols (TAGs), while they can be precursors or intermediates in the biosynthesis of TAGs, glycerophospholipids, and glyceroglycolipids.[1] DAGs also serve as signaling molecules.[2] For example, DAG accumulation is associated with activation of protein kinase C in skeletal muscle and liver cells, which ultimately influences downstream insulin signaling.[3] Abnormal accumulation of DAGs has been reported in disease states associated with insulin resistance, such as cardiac hypertrophy,[4] diabetes,[5] and cardiac lipotoxicity.[6] Recently, plasma DAG composition has been used as a biomarker of metabolic syndrome onset in rhesus monkeys.[7]

In terms of DAG profiling, gas chromatography–mass spectrometry (GC-MS) is a traditionally used technique.[8] In this workflow, DAGs need to be separated from other lipid classes and subsequently derivatized (e.g., trimethylsilyl ethers) to increase their volatility.[9] The overall process requires relatively large sample amount and long analysis time. More recently, high-performance liquid chromatography (HPLC)-MS has been increasingly applied to DAG analysis. DAGs together with other neutral lipids can be well-separated on the column, allowing quantitation of 1,2-DAG and 1,3-DAG *sn*-isomers from complex mixtures.[10] The advancement of electrospray ionization-tandem mass spectrometry (ESI-MS/MS) of lipids has facilitated global lipid analysis without the need of a prior lipid class separation, coined as “shotgun lipid analysis” by Han and Gross.[11] Shotgun analysis has the advantages of fast analysis speed and the capability of detecting a broad range of lipid classes, which has found increasing applications in biomedical discoveries.[12] Per the nonpolar nature, DAGs are detected as adduct ions, viz. $[DAG + X]^+$ ($X = Li^+$, Na^+, NH_4^+) by ESI.[13,14] Collision-induced dissociation (CID) of the ammonium adduct ions forms abundant fatty acyl specific fragment ions (as combined loss of NH_3 and free fatty acid), allowing the assignment of DAG structures.[13] An obvious drawback of using adduct ion formation in DAG analysis is that the ionization efficiency is not high, which also varies according to the fatty acyl chain lengths and the degree of unsaturation.[15,16] These variations require the use of multiple DAG internal standards for quantitation.[13]

Charge derivatization is an effective approach to boost ionization efficiency of neutral lipids via ESI-MS.[17] Established derivatization methods target the free hydroxyl group in DAGs through ester bond formation with a charge reagent. This strategy also blocks potential fatty acyl migration in DAGs.[18] *N*-Chlorobetainyl chloride,[19] *N,N*-dimethylglycine (DMG),[18] and DMG imidazolide[20] have been demonstrated as efficient charge derivatization reagents, enhancing the ion signal of DAGs by at least 2 orders of magnitude than forming their adduct ions.[19] CID of charge derivatized DAGs typically produces tag specific fragment in high abundance, facilitating the development of MS/MS transitions for sensitive quantitation (limit of quantitation (LOQ), 100 pM via DMG derivitization).[18] Because fatty acyl chain specific fragment ions are absent from direct CID of the charge tagged DAGs, adduct formation of the derivatized DAGs with Li^+ or NH_4^+ is still needed for structural elucidation. This approach although requires the addition of salt into ESI solution, the Han group demonstrated that it provided a distinct benefit of quantifying the *sn*-1,2- and 1,3-isomers based on CID of lithiated DMG-DAG ions.[18]

In biological systems, a substantial proportion of DAGs consists of unsaturated fatty acyls. As an example, the concentration of unsaturated DAGs was found to be ~0.81 μM out of ~0.88 μM, the total DAG concentration in human plasma; that is, 92% of DAGs are unsaturated.[21] Given the prevalence of unsaturated DAGs in lipidomes, we are interested in exploring alternative charge derivatization methods that target the carbon–carbon double bond (C=C) as a site for the introduction of a charge tag. Recently, we have demonstrated thiyl radical tagging for sterol lipid analysis by linking an ionizable thiol reagent (thioglycolic acid, TGA) to the unsaturated B ring in sterols.[22] This derivatization when coupled with ESI-MS/MS via low energy CID provided rapid (in minutes) and sensitive quantitation (limit of detection (LOD) in nM) of sterols from complex mixtures.

Thiol–ene coupling reaction, involving thiyl radical addition to an alkene function group, is a widely adopted methodology for the formation of carbon–sulfur bonds.[23] It fulfills the “click-chemistry” paradigm of high reaction rates, quantitative conversion in mild condition, and simple workup procedures (i.e., removal of byproducts by nonchromatographic methods).[24] Thiol–ene chemistry has found broad applications in polymer and material synthesis,[25] surface functionalization,[26] and drug delivery.[27]

Taking advantage of its high specificity for C=C transformation, herein we explored a charge derivatization strategy based on thiol–ene chemistry to tag the C=C in unsaturated DAGs as illustrated in Scheme 1a. The success of the tagging would allow enhanced sensitivity of the DAGs via ESI-MS. Moreover, the newly formed C–S bond in the derivatized DAG species is less likely to be a facile dissociation site under charge driven fragmentation conditions due to the relatively nonpolar nature of the C–S bond. This property should facilitate the formation of structural informative fragment ions, that is, fatty acyl chain related fragments. In this work, synthetic DAG standards with varying chain lengths and degrees of unsaturation were used for method development, including optimizing reaction conditions, screening for suitable thiol compounds as charge tags, and developing MS/MS methods for identification and quantitation. The analytical capability of the established method was demonstrated by performing analysis of DAGs from human plasma samples of type 2 diabetes mellitus (DM) patients using a shotgun lipidomic approach.

EXPERIMENTAL SECTION

Lipid Nomenclature

Shorthand notations for glycerolipids are based on the guidelines provided by LIPID MAPS.[28] For synthetic lipid standards with known *sn* positions, "/" separator is used such as in DAG 16:0/18:1/0:0 to represent DAG consisting of C16 and C18 fatty acyls at *sn*-1 and *sn*-2 positions, respectively. DAG 16:0/0:0/18:1 stands for a DAG with C16 and C18 fatty acyls at *sn*-1 and *sn*-3 positions, respectively. 0:0 represents no fatty acyl chain is linked. The "0" and "1" after the carbon number represents the degree of unsaturation. The interchangeable "_" notation, such as in DAG 16:0_18:1, is adopted for DAG with unidentified *sn* positions.

Materials

All the chemical reagents and solvents were purchased from commercial sources and were used without further purification. DAGs 16:0/18:1(9Z)/0:0, 15:0/18:1-d_7(9Z)/0:0, 18:0/20:4(5Z,8Z,11Z,14Z)/0:0, 18:1(9Z)/18:1(9Z)/0:0, and 18:1(9Z)/0:0/18:1(9Z) were purchased from Avanti Polar Lipids Inc. (Alabaster, AL, USA). DAGs 14:1(9Z)/14:1(9Z)//0:0, 16:1(9Z)//16:1(9Z)//0:0, 17:1(9Z)/17:1(9Z)/0:0, 18:1(6Z)/18:1(6Z)/0:0, 18:2-(9Z,12Z)/18:2(9Z,12Z)/0:0, 18:3(9Z,12Z,15Z)/18:3-(9Z,12Z,15Z)/0:0, 20:1(9Z)/20:1(9Z)/0:0, 22:1(9Z)/22:1(9Z)/0:0, and 24:1(9Z)/24:1(9Z)/0:0 were purchased from Nu-Check Prep, Inc. (Elysian, MN, USA). Thioglycolic acid (TGA), sodium-2-mercaptoethanesulfonate (MESNA), cysteamine (CA) hydrochloride, dimethylformamide (DMF), 2,2-dimethoxy-2-phenylacetophenone (DMPA), hydrochloric acid, and ethyl acetate were purchased from Sigma-Aldrich (St. Louis, MO, USA). Deionized water was obtained from a purification system at 0.03 $\mu S \cdot cm$ (model: Micropure UV; Thermo Scientific; San Jose, CA, USA). Pooled human plasma (Li Heparin used as anticoagulant) was purchased from Innovative Research (Novi, MI, USA).

Human Plasma Sample Collection

Six human plasma samples, including 3 healthy normal controls and 3 type 2 DM patients were collected from Affiliated Dongfeng Hospital, Hubei University of Medicine (Shyian, Hubei Province, China).

Lipid Extraction

The procedure for total lipid extraction from plasma (Section 1, Supporting Information) was based on established protocols.[29,30] Briefly, 50 μL of plasma, 0.3 mL of 0.67 M phosphate buffer solution, and 2.0 mL of chloroform–methanol (3:1, v/v) were combined in 100 mm × 13 mm glass test tubes. The mixture was vortex-mixed for 2 min and then was centrifuged at 1200 g for 5 min for phase separation. The aqueous layer was removed using a glass Pasteur pipet, while the remaining organic layer was transferred to another glass test tube and was dried under a stream of nitrogen gas. For quantitative analysis, DAGs were fractioned from other classes of lipids using a 100-mg Isolute silica cartridge (Biotage, Charlotte, NC, USA). The lipid extracts were stored at −20 °C until further analysis.

Derivatization of DAG Standards, Plasma Lipid Extract, and Plasma

DAG (0.01–200 μM), thiol reagent (100 mM), and DMPA (photoinitiator, 0.5 mM), were dissolved in DMF and degassed with nitrogen gas before photochemical reactions. The solution was pumped through a flow microreactor (in μL/min flow rate range), made from UV transparently coated fused silica capillary (100 μm i.d., 375 μm o.d.; Polymicro Technologies; Phoenix, AZ, USA). A low-pressure mercury lamp with an emission band at 351 nm (model number: 80–1057–01/351; BHK, Inc.; Ontario, CA, USA) was placed in parallel to the capillary at a distance of 0.5 cm. This whole setup was enclosed in a cardboard box to prevent stray light. At the exit of the microflow reactor, the reaction solution (100 μL) was collected in a glass vial and added with ethyl acetate (200 μL). The mixture was washed twice with 0.1 M aq. HCl (400 μL) to remove excess thiol reagent (e.g., CA) before MS analysis. The same procedure was applied to direct derivatization of lipids in plasma (1–20 μL) without a prior lipid extraction step.

MS Analysis of Neutral Lipid Standards and Lipid Extracts

MS analysis of charge derivatized DAG standards and lipid extracts were performed on a 4000 QTRAP and a 4500 QTRAP mass spectrometer (SCIEX, Toronto, ON, CA) equipped with a home-built nanoESI source (pulled borosilicate glass emitters). Optimized MS parameters were as follows: nanoESI spray voltage: ± (1400–1800) V; curtain gas: 10 psi; declustering potential: ± 20 V; a scan rate of 1000 Da/s for 4000 QTRAP and 10 000 Da/s for 4500 QTRAP. The instrument was used in a linear ion trap MS analysis mode or in triple quadrupole linked scan mode (precursor ion scan (PIS) or neutral loss scan (NLS)).[31]

RESULTS AND DISCUSSION

Charge Tagging via Thiol–ene Chemistry

Scheme 1a shows a classic view of thiol–ene reaction with an unsaturated lipid depicted for the conventional alkene.[24] Briefly, upon exposure to 351 nm UV irradiation, DMPA (the photoinitiator, PI) undergoes Norrish Type I cleavage to generate benzoyl radical and 1,1-dimethoxy-1-phenylmethyl radical. These carbon-centered radicals abstract the sulfur–hydrogen in the thiol reagent, forming alkylthiyl radical. The thiyl radical then adds to the C=C to form a carbon-centered radical, which subsequently abstracts a hydrogen atom from another thiol molecule to produce the derivatized product, while the newly formed thiyl radical propagates in the radical chain process. Thiol–ene reactions are not regioselective for internal double bonds; so two regio-isomers resulting from the addition to either carbon in the original C=C are formed.[32]

Using DAG 16:0/18:1/0:0 as a model compound, three thiol reagents, TGA, MESNA, and CA (structures shown in Scheme 1b), were tested for thiol–ene charge tagging. These thiols were selected based on the presence of readily ionizable functional group either for protonation or deprotonation under typical ESI conditions, reasonable solubility, and commercial availability. Moreover, it was preferred that the charge tagged DAG ions could generate structurally informative fragment ions upon CID. DMPA, a commonly used photoinitiator for thiol–ene reactions was adopted here, while DMF was used as the reaction solvent.[23] Prior to MS analysis, a simple wash procedure was performed to reduce signal

suppression from remaining thiol reagent. The reaction progress was monitored through the intensity of tagged DAG ions via nanoESI-MS.

Figure 1a–c summarizes the postreaction nanoESI-MS spectra of DAG 16:0/18:1/0:0 (1 μM) resulting from three individual thiol reagents after reaching equilibrium. A single reaction product was detected at high ion intensities (counts per second, cps) from each reagent, that is, *m/z* 685.5 ($[^{TGA-}DAG - H]^-$), *m/z* 735.4 ($[^{MESNA-}DAG - H]^-$), *m/z* 672.5 ($[^{CA-}DAG + H]^+$) from TGA and MESNA in negative ion mode, and CA in positive ion mode, respectively. The mass differences (insets in Figure 1) between the detected products and the DAG molecule (594.2 Da) match well with the mass of the corresponding thiol reagent, suggesting successful thiol–ene coupling. Moreover, all three thiol reagents significantly improved ionization of DAG in nanoESI. Using CA as an example, the ion intensity of CA tagged DAG was 10 times higher than its ammonium adduct (Figure S1).

The data in Figure 1d represent typical MS^2 beam-type CID (CE = 35 V) of TGA derivatized DAG anions (*m/z* 685.5) in negative ion mode. Different from CID of TGA derivatized sterols,[22] 44 Da loss ($-CO_2$) from TGA carboxylic group was not observed; neither was the tag loss. Instead, the fatty acyl anions, including $[C16:0–H]^-$ (*m/z* 255.3) and $[^{TGA-}C18:1\text{-}CO_2–H]^-$ (*m/z* 329.2, a sequential loss of CO_2 from the TGA tag) were quite abundant. Beam-type CID of MESNA derivatized DAG anions (CE = 60 eV, Figure 1e) produced three major fragments, neutral loss of C16:0 (*m/z* 479.2), thiol tagged C18:1 anions ($[^{MESNA-}C18:1\text{-}CO_2–H]^-$, *m/z* 423.2), and $[C16:0–H]^-$ (*m/z* 255.3). Clearly, CID of TGA and MESNA tagged DAG anions readily allow identification of fatty acyl composition in DAG.

Beam-type CID spectrum of protonated ^{CA-}DAG (Figure 1 f, CE = 32 V) is rather simple with three fragment peaks produced present at almost equal abundance. The fragment peak at *m/z* 577.5 resulted from sequential loss of CA tag (77 Da) and H_2O (18 Da), leading to a characteristic neutral loss of 95 Da. The fragment ions at *m/z* 339.5 and 313.5 derived from sequential loss of CA tag and the fatty acyl chains, C18:1 and C16:0, respectively. The above sequences of fragmentation were supported by accurate mass measurement and MS^3 CID experiments (Figures S2 and S3). The possible structures for the observed major fragments are presented in Scheme 2, while possible fragmentation pathways are proposed in Schemes S1–S5.

Although the three thiol reagents all delivered improved ionization and useful structural information (fatty acyl chain composition) upon CID, we decided to choose CA for further method development. This is because, besides the fatty acyl information, the distinct 95 Da neutral loss associated with the CA tag facilitates the development of NLS for detection and quantitation of DAGs from mixtures.

Optimization of CA Thiol–ene Coupling

In synthetic settings, the thiol reagent is typically placed in stoichiometric relationship to the alkenes in thiol–ene reactions.[23] Although the concentrations of DAGs in biological samples are typically at sub-μM level or lower, it is necessary to use high concentrations of PI and thiol reagent (both in mM) to maintain adequate steady-state concentrations of the thiyl

radical so as to sustain radical chain reactions depicted in Scheme 1a. For instance, reactions involving 10 mM CA, 0.5 mM DMPA, and 5 μM DAG 16:0/18:1/0:0 produced a major product at *m/z* 670.5, two Da less than the expected thiol–ene coupling product (Figure S4). This type of product has been observed in polymer synthesis and identified by NMR to have a shifted C=C in the structure.[33] By increasing the concentration of CA to 100 mM or higher, this side product could be effectively reduced to less than 2% of the thiol–ene coupling product. Although higher concentrations of CA led to faster and cleaner reactions, there was no significant benefit to increase CA concentrations over 100 mM. With the use of a flow microreactor, CA tagging could be accomplished within 40 s for a variety of DAGs consisting of different lengths of fatty acyls and different numbers of C=Cs. The representative kinetic curves can be found in Figures S5 and S6, Supporting Information.

Polyunsaturated DAGs

For DAGs consisting of polyunsaturated fatty acyls, we wondered if multiple tagging could happen. Figure 2 summarizes the postreaction spectra of DAG 15:0/18:1-d_7/0:0, DAG 18:3/18:3/0:0 and DAG 18:0/20:4/0:0, which were derivatized separately but under identical reaction conditions using the flow microreactor setup. The production of mono-CA tagging products reached steady state within 1 min of UV exposure. Despite the presence of multiple C=Cs in the latter two DAGs, only single CA tagging products were observed (*m/z* 690.3 and 722.3), same as the tagging of DAG 15:0/18:1-d_7/0:0 (*m/z* 665.3), which has one C=C in the molecule. It is worth noting that no doubly charged ions corresponding to sequential tagging were present in the lower mass range (Figure S7). Irradiation of reaction mixture with UV for 1 h in bulk processes, led to <10% of second tagging (Figure S8). Under the same reaction condition, derivatization using TGA produced >35% of second tagging products of DAG 18:1/18:1/0:0 (Figure S9). Such difference can be attributed to the higher reactivity of TGA than CA.[34] Although the preferred formation of mono-CA tagging products in the polyunsaturated system is not fully understood at this moment, the phenomenon nonetheless is advantageous for sensitive detection and quantitation in subsequent MS/MS experiments.

The CA derivatized DAG species was further analyzed by MS/MS via beam-type CID (Figure 2d–f). Upon CID (CE = 32 V), fragments corresponding to sequential loss of CA and fatty acyl chains are consistently observed with high intensities.

However, the relative intensity of the 95 Da loss (the combined loss of CA and H_2O) decreases as the degree of unsaturation in a fatty acyl chain increases, for example, C20:4 < C18:3 < C18:2 < C18:1. This aspect suggests that the application of 95 Da NLS to the polyunsaturated system may have a lower sensitivity than the ones consisting lower degree of unsaturation in the fatty acyl chains. In this case, NLS targeted for a specific polyunsaturated fatty acyl chain, for example, 381 Da NLS for the combined losses of CA (77 Da) and C20:4 (304 Da), can be used to get around this problem and achieve sensitive detection. Table S2 summarizes the combined loss of CA and various fatty acyl chains present in DAGs.

DAG *sn*- and C=C Positional Isomers

We also explored the potential of differentiating *sn*- and C=C positional isomers of DAGs via CA tagging and subsequent CID. For instance, *sn*-1,2- and 1,3-DAG 18:1(9Z)/18:1(9Z) were derivatized by CA and analyzed. Unfortunately, the MS/MS spectra for the two *sn*-isomers were identical and thus, did not provide any distinction (Figure S10). CID of CA tagged DAG 18:1(6Z)/18:1(6Z)/0:0 showed similar fragmentation pattern to DAG 18:1(9Z)/18:1(9Z)/0:0 (data not shown). Therefore, no distinction on the C=C location was achieved from CA tagging and CID.

Quantitative Analysis

It has been shown that the ionization response of DAGs in alkali metal adduct forms are highly dependent on chain lengths and the degrees of unsaturation of fatty acyls.[13] Here we examined if such bias also existed for DAGs after CA tagging. Nine unsaturated DAGs (equal molar, 1 μM each) with fatty acyls varying from C28 to C48 and degrees of unsaturation in the range of 1 to 4 were mixed together, while 0.5 μM DAG 15:0/18:1-d_7/0:0 was added as the internal standard (IS). This mixture was then subjected to CA derivatization for 1 min using the flow microreactor setup. Figure 3a shows the postreaction nanoESI-MS spectrum. The derivatized DAG species yielded similar ion response regardless of the change of fatty acyl chain length and unsaturation. The relative standard deviation (16%, $n = 3$) of the DAG signals are within the expected errors arising from sample handling. The above results suggest that CA tagging can successfully minimize ionization bias for DAGs in ESI due to variations in fatty acyl composition. Moreover, signal suppression among DAGs during mixture analysis is very limited.

We further assessed the performance of 95 Da NLS for DAG quantitation. A good linear correlation ($R^2 = 0.9981$) was achieved between MS response and concentration (DAG 16:0/18:1/0:0, 0.1–2 μM) by employing 1.0 μM DAG 15:0/18:1-d_7/0:0 as IS (Figure 3b and c). Since monotagging was dominant for DAGs consisting of multiple C=Cs, 95 Da NLS also provided good linear correlations for their quantitation (Table S1). The LOD for DAG 16:0/18:1/0:0 could be achieved at 100 pM from 95 Da NLS (S/N 3:1, Figure 3d). Such level of LOD is comparable to values reported from other charge derivatization approaches, for example, LOQ of 100 pM using DMG via ESI-MS/MS[18] and LOD of 10 nM using *N*-chlorobetainyl chloride via ESI-MS.[19] Overall, CA tagging of DAG followed by ESI-MS/MS enjoys the benefits of fast analysis (less than 2 min per run) and sensitive detection.

Analysis of DAGs from Human Plasma

The analysis of DAGs from crude mixture is often hindered from their relatively low abundance (~0.88 μM) and ion suppression from other neutral lipids, such as CEs (~3.5 mM) and TAGs (~1.0 mM).[21] Conventional analytical methods typically involve multistep liquid–liquid extraction, enrichment and/or chromatographic separation before MS. Herein, we tried to achieve rapid and sensitive analysis of DAGs by thiol–ene derivatization without resorting to chromatographic separation on clinical human plasma samples. As a demonstration, 1 μL of human plasma was directly subjected to CA derivatization (1 μM of DAG 15:0/18:1-d_7/0:0 added as IS). Figure 4a shows the postreaction nanoESI-MS spectrum. Three classes of neutral lipids were detected, representing CA tagged CEs, DAGs,

and TAGs. These assignments were based on the detected monoisotopic *m/z* values and corresponding MS/MS data. For instance, the peak at *m/z* 726.9 was identified as $^{CA-}$CE 18:2. CID of this peak produced a dominant fragment peak at *m/z* 369 (cholestene cations) due to sequential loss of CA and C18:2 from the tagged CE. Similarly, ions at *m/z* 962.8 were identified as $^{CA-}$TAG 18:1/18:1/18:1 based on the detection of sequential loss of CA and C18:1 (Figure S12).

As expected, CA tagged DAGs were detected at low intensities as compared to CEs and DAGs in the MS^1 spectrum (Figure 4a). However, by using 95 Da NLS, 7 distinct DAG molecular species were observed (Figure S12). The above data clearly demonstrate the capability of CA tagging followed by 95 Da NLS for selective detection of DAGs even at the presence of other more abundant neutral lipids. We further examined if unsaturated phosphocholines (PCs) would be tagged by CA given their relatively high abundance in plasma. It turned out that PC had very low reactivity toward CA; CID of the CA tagged PC ions presented different fragmentation pattern from that of $^{CA-}$DAG ions (Figure S13). Therefore, the presence of unsaturated PCs would not interfere with DAG detection.

For quantitative analysis DAGs were extracted and purified from 50 μL of human plasma (recovery rate = 94 ± 3%). Eleven peaks of $^{CA-}$DAGs were detected from 95 Da NLS (Figure 4b). MS/MS analysis proved that many DAGs consisted of fatty acyl compositional isomers. For example, CID of ions at *m/z* 644.2, $^{CA-}$DAG 32:1, showed abundant losses of 359 Da (CA + C18:1), 333 Da (CA + C16:0), 331 (CA + C16:1), and 305 Da (CA + C14:0), corresponding to product ions at *m/z* 285, 311, 313, and 339, respectively (Figure 5c). Based on the number of fatty acyl carbon atoms and double bonds, DAG 32:1 was assigned to contain two fatty acyl compositional isomers: DAG 14:0_18:1 and DAG 16:0_16:1. Similarly, DAG 34:2 (the peak at *m/z* 670.2 in Figure 4b) contained DAG 16:1_18:1 and DAG 16:0_18:2 (Figure S15). In order to assess the relative change of the distinct DAG species within the parent ion, fatty acyl chain specific NLS and PIS can also be employed (Figure S16). PIS of 339 and 337 Da revealed the existence of DAGs containing C18:1 and C18:2, respectively. Overall, 18 distinct DAG species were identified to the level of fatty acyl composition as summarized in Table 1. Quantitative analysis of DAGs from the pooled human plasma was performed using 95 Da NLS. Calibration curves for each individual DAG species were obtained using DAG 15:0/18:1-d_7/0:0 (1 μM) as IS (Table S1). These values fall within the range of reported unsaturated DAGs measured from human plasma using HPLC-MS/MS.[21] However, since CA tagging is specific for unsaturated DAGs, saturated DAGs (e.g., DAG 16:0/16:0) could not be detected. Besides, CA tagging followed by CID cannot differentiate *sn*-isomers.

DAG Analysis of Type 2 Diabetes Mellitus Human Plasma

Various studies have shown the correlation of increased intracellular DAG content in liver and muscle in type 2 DM.[35] Recently, Shaw et al. have demonstrated aberration of plasma lipidome occurs prior to the onset of type 2 DM.[36] We were interested to test if CA tagging followed by 95 Da NLS was capable in providing quick profiling of DAGs in plasma for type 2 DM patients. Figure 5 summarizes the relative intensity changes of unsaturated DAGs relative to IS (DAG 15:0/18:1-d_7/0:0, 1 μM) from two sets of samples (normal controls, N =

3; DM patients, *N* = 3). Representative 95 Da NLS spectra can be found in Figure S14. The major DAG species include DAG 34:2, 34:1, 36:3, and 36:2. The relative intensities of DAG 34:2, 34:1, and 36:2 decreased by 2.5 ± 0.7, 2.8 ± 1.1, and 1.6 ± 0.4 times in DM patients as compared to the control, respectively. However, DAG 36:4 in the DM patients increased by 5 ± 2 times relative to the control. In terms of the change of fatty acyl compositional isomers, CID of $^{CA-}$DAG 36:2 revealed a reduction of DAG 16:0_18:1 relative to isomer DAG 16:0_18:2 in DM patients (Figure S17). Further studies are required with the use of a larger sampling size and controlled medication of the type 2 DM patients.

CONCLUSIONS

In this study, we have utilized thiol–ene click chemistry as an effective charge derivatization method to enable fast analysis of unsaturated DAGs by nanoESI-MS. Cysteamine (CA) was identified as a proper derivatization reagent, which allowed fast charge tagging (in 1 min) and enhanced ionization (by 10 times) of a variety of unsaturated DAGs as compared to conventional adduct ion formation. Low-energy CID of CA tagged DAGs led to simple product ion spectrum, yet rich in structural information. Specifically, the combined neutral loss of the tag (CA) and fatty acyls (RCOOH) readily allowed the assignment of fatty acyl chains, leading to confident identification of multiple fatty acyl compositional isomer of DAGs in biological samples. The other major fragmentation channel was the combined loss of CA and H_2O (95 Da). On the basis of this characteristic loss, 95 Da NLS was established as a sensitive means for detection (LOD of 100 pM) and quantitation of unsaturated DAGs. The above method was further applied to DAG analysis of pooled human plasma and plasma samples from type 2 DM patients. In comparison with methods based on GC-MS and HPLC-MS for DAG analysis, CA tagging followed by ESI-MS/MS has several advantages, such as fast analysis speed (2 min vs up to 60 min for analysis) and the potential of direct analysis of small quantity of clinical sample (e.g., 1 μL plasma). In terms of limitations, this method cannot analyze saturated DAGs and it is not capable to provide *sn*-position information. Preliminary LC-MS data showed multiple or broadened elution peaks resulting from mono-CA tagging of DAGs having more than one C=C, likely due to formation of multiple regio-isomers (Figure S19). This phenomenon suggests that CA tagging could increase the complexity for mixture analysis when coupled with LC-MS. CA tagging for DAG analysis is just one example of applying thiol–ene click chemistry to solve a specific analytical problem, viz. DAG analysis. As shown in the example of direct analysis of human plasma, other classes of unsaturated neutral lipids (CEs and TAGs) were also detected. In future studies, we plan to expand the thiol–ene derivatization toolbox and develop methods to enhance analysis of other important neutral lipids.

Supplementary Material

Refer to Web version on PubMed Central for supplementary material.

Acknowledgments

Financial support from National Natural Science Foundation of China (No. 21722506, No. 21621003) and NIH R01GM118484 is greatly appreciated.

References

1. Goñi FM, Alonso A. Prog Lipid Res. 1999; 38:1–48. [PubMed: 10396601]
2. Colón-González F, Kazanietz MG. Biochim Biophys Acta, Mol Cell Biol Lipids. 2006; 1761:827–837.
3. Erion DM, Shulman GI. Nat Med. 2010; 16:400–402. [PubMed: 20376053]
4. Arimoto T, Takeishi Y, Takahashi H, Shishido T, Niizeki T, Koyama Y, Shiga R, Nozaki N, Nakajima O, Nishimaru K. Circulation. 2006; 113:60–66. [PubMed: 16380548]
5. Eichmann TO, Lass A. Cell Mol Life Sci. 2015; 72:3931–3952. [PubMed: 26153463]
6. Drosatos K, Schulze PC. Curr Heart Failure Rep. 2013; 10:109–121.
7. Polewski MA, Burhans MS, Zhao M, Colman RJ, Shanmuganayagam D, Lindstrom MJ, Ntambi JM, Anderson RM. J Lipid Res. 2015; 56:1461–1470. [PubMed: 26063458]
8. Murphy RC, Fiedler J, Hevko J. Chem Rev. 2001; 101:479–526. [PubMed: 11712255]
9. Tserng K-Y, Griffin R. Anal Biochem. 2003; 323:84–93. [PubMed: 14622962]
10. Leiker TJ, Barkley RM, Murphy RC. Int J Mass Spectrom. 2011; 305:103–108. [PubMed: 21860599]
11. Han, X. Lipidomics Comprehensive Mass Spectrometry of Lipids. John Wiley & Son, Inc; Hoboken, NJ: 2016.
12. Han X. Biochim Biophys Acta, Mol Cell Biol Lipids. 2017; 1862:804–807.
13. Murphy RC, James PF, McAnoy AM, Krank J, Duchoslav E, Barkley RM. Anal Biochem. 2007; 366:59–70. [PubMed: 17442253]
14. Bowden JA, Albert CJ, Barnaby OS, Ford DA. Anal Biochem. 2011; 417:202–210. [PubMed: 21741949]
15. Li X, Evans JJ. Rapid Commun Mass Spectrom. 2005; 19:2528–2538. [PubMed: 16106375]
16. Li X, Collins EJ, Evans JJ. Rapid Commun Mass Spectrom. 2006; 20:171–177. [PubMed: 16331741]
17. Wang M, Wang C, Han RH, Han X. Prog Lipid Res. 2016; 61:83–108. [PubMed: 26703190]
18. Wang M, Hayakawa J, Yang K, Han X. Anal Chem. 2014; 86:2146–2155. [PubMed: 24432906]
19. Li YL, Su X, Stahl PD, Gross ML. Anal Chem. 2007; 79:1569–1574. [PubMed: 17297957]
20. Johnson DW. J Mass Spectrom. 2001; 36:277–283. [PubMed: 11312519]
21. Quehenberger O, Armando AM, Brown AH, Milne SB, Myers DS, Merrill AH, Bandyopadhyay S, Jones KN, Kelly S, Shaner RL, Sullards CM, Wang E, Murphy RC, Barkley RM, Leiker TJ, Raetz CR, Guan Z, Laird GM, Six DA, Russell DW, et al. J Lipid Res. 2010; 51:3299–3305. [PubMed: 20671299]
22. Adhikari S, Xia Y. Anal Chem. 2017; 89:12631–12635. [PubMed: 29155553]
23. Hoyle CE, Bowman CN. Angew Chem, Int Ed. 2010; 49:1540–1573.
24. Hoyle CE, Lee TY, Roper T. J Polym Sci, Part A: Polym Chem. 2004; 42:5301–5338.
25. Lowe AB. Polym Chem. 2014; 5:4820–4870.
26. Resetco C, Hendriks B, Badi N, Du Prez F. Mater Horiz. 2017; 4:1041–1053.
27. Meghani NM, Amin HH, Lee B-J. Drug Discovery Today. 2017; 22:1604–1619. [PubMed: 28754291]
28. Liebisch G, Vizcaíno JA, Köfeler H, Trötzmüller M, Griffiths WJ, Schmitz G, Spener F, Wakelam MJO. J Lipid Res. 2013; 54:1523–1530. [PubMed: 23549332]
29. Folch J, Lees M, Stanley GHS. J Biol Chem. 1957; 226:497–509. [PubMed: 13428781]
30. Ingalls ST, Kriaris MS, Xu Y, Dewulf DW, Tserng KY, Hoppel CL. J Chromatogr, Biomed Appl. 1993; 619:9–19.
31. Hager JW. Rapid Commun Mass Spectrom. 2002; 16:512–526.
32. Turunc O, Firdaus M, Klein G, Meier MAR. Green Chem. 2012; 14:2577–2583.
33. Mutlu H, Parvulescu AN, Bruijnincx PCA, Weckhuysen BM, Meier MAR. Macromolecules. 2012; 45:1866–9297.
34. Hong M, et al. J Polym Sci, Part A: Polym Chem. 2012; 50:2499–2506.

35. Szendroedi J, Yoshimura T, Phielix E, Koliaki C, Marcucci M, Zhang D, Jelenik T, Müller J, Herder C, Nowotny P, Shulman GI, Roden M. Proc Natl Acad Sci U S A. 2014; 111:9597–9602. [PubMed: 24979806]

36. Meikle PJ, Wong G, Barlow CK, Weir JM, Greeve MA, MacIntosh GL, Almasy L, Comuzzie AG, Mahaney MC, Kowalczyk A, Haviv I, Grantham N, Magliano DJ, Jowett JBM, Zimmet P, Curran JE, Blangero J, Shaw J. PLoS One. 2013; 8:e74341. [PubMed: 24086336]

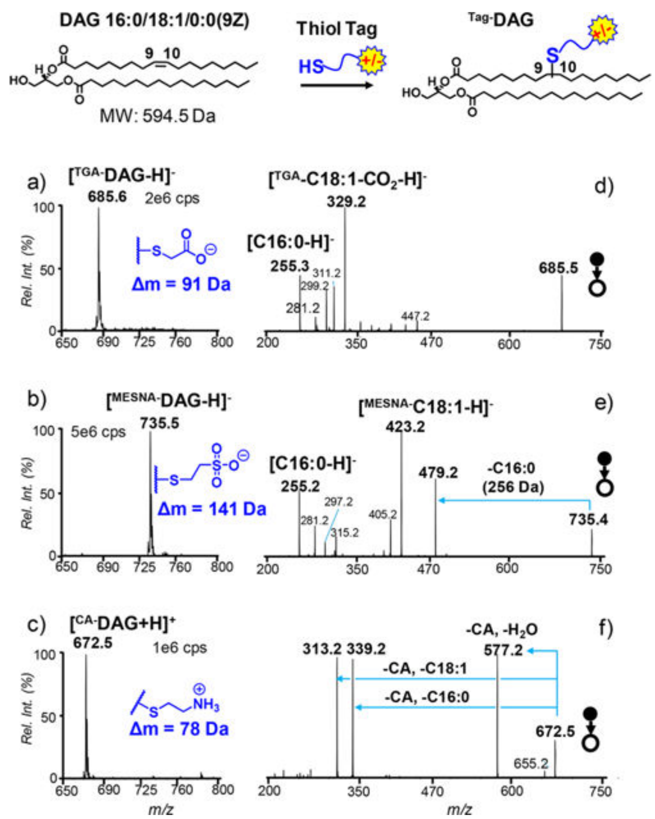

Figure 1.

Charge tagging of DAG 16:0/18:1(9Z)/0:0 (1 *μ*M) using thiol–ene chemistry. The inset at the top shows a generic reaction scheme for charge tagging. Post reaction nanoESI MS spectra after derivatization with (a) TGA and (b) MESNA in negative ion mode, and (c) CA in positive ion mode. MS^2 beam-type CID of (d) ^{TGA}-DAG at *m/z* 685.5 (CE = 35 V) in negative ion mode, (e) ^{MESNA}-DAG at *m/z* 735.4 (CE = 60 V) in negative ion mode, and (f) $^{CA-}$DAG at *m/z* 672.5 (CE = 32 V) in positive ion mode.

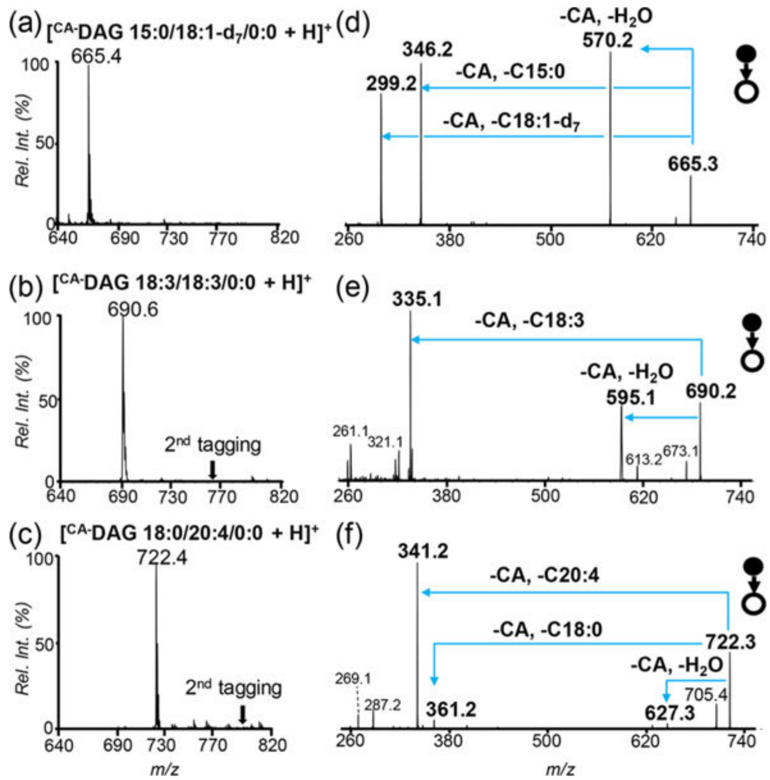

Figure 2.

Post-CA tagging nanoESI MS spectra of (a) DAG 15:0/18:1-d_7/0:0, (b) DAG 18:3/18:3/0:0, and (c) DAG 18:0/20:4/0:0.MS^2 beam type CID (CE 32 V) of (d) $^{CA-}$DAG 15:0/18:1-d_7/0:0 (*m/z* 665.3), (e) $^{CA-}$DAG 18:3/18:3/0:0 (*m/z* 690.2), and (f) $^{CA-}$DAG 18:0/20:4/0:0 (*m/z* 722.3).

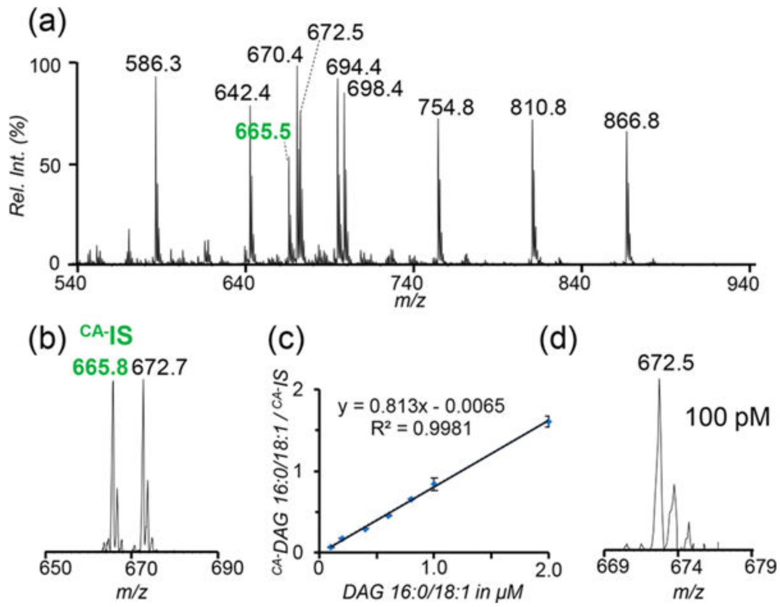

Figure 3.

(a) Post-CA tagging nanoESI MS spectrum of equimolar (1 *μ*M each) mixture of DAG 14:1/14:1/0:0 (*m/z* 586.3), 16:1/16:1/0:0 (*m/z* 642.4), 17:1/17:1/0:0 (*m/z* 670.4), 16:0/18:1/0:0 (*m/z* 672.5), 18:2/18:2/0:0 (*m/z* 694.4), 18:1/18:1/0:0 (*m/z* 698.4), 20:1/20:1/0:0 (*m/z* 754.8), 22:1/22:1/0:0 (*m/z* 810.8), and 24:1/24:1/0:0 (*m/z* 866.8), with 0.5 *μ*M of IS (15:0/18:1-d_7/0:0, *m/z* 665.5). (b) 95 Da NLS of $^{CA-}$DAG 16:0/18:1/0:0 (1 *μ*M) and IS (1 *μ*M). (c) A linear plot resulted from 95 NLS for DAG 16:0/18:1/0:0 (R^2 = 0.9981). Error bars represent standard deviation; *n* = 3. (d) 95 Da NLS of 100 pM DAG 16:0/18:1/0:0 after CA tagging.

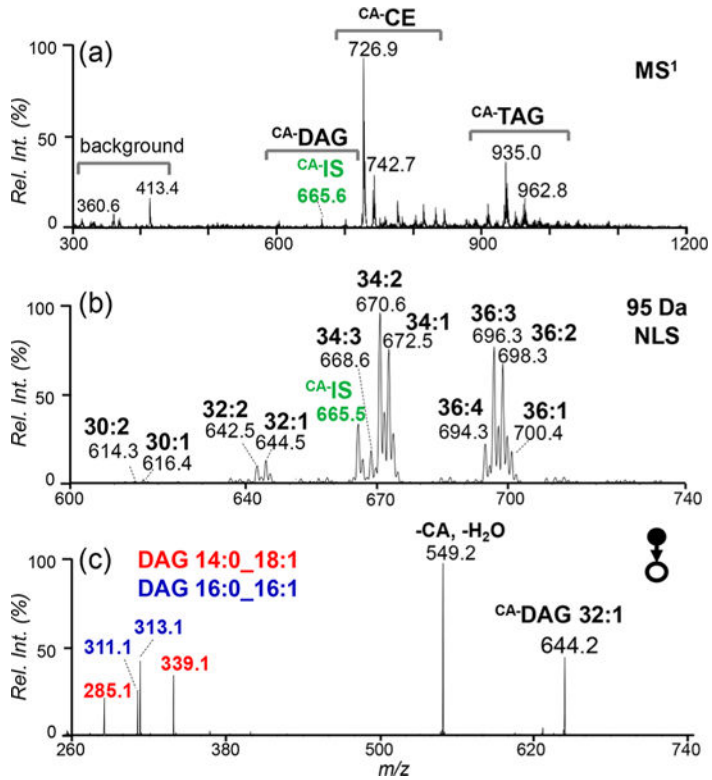

Figure 4.

(a) Post-CA tagging nanoESI mass spectrum of 1 μL pooled human plasma with 1 μM DAG 15:0/18:1-d$_7$/0:0 added as the IS. The *m/z* regions correspond to tagged neutral lipid classes are indicated. (b) 95 Da NLS for unsaturated DAGs (mass range *m/z* 600–740). (c) MS^2 CID of *m/z* 644.2 ([$^{CA-}$DAG 32:1 + H]$^+$) reveals two fatty acyl composition isomers, DAG 14:0_18:1 and DAG 16:0_16:1.

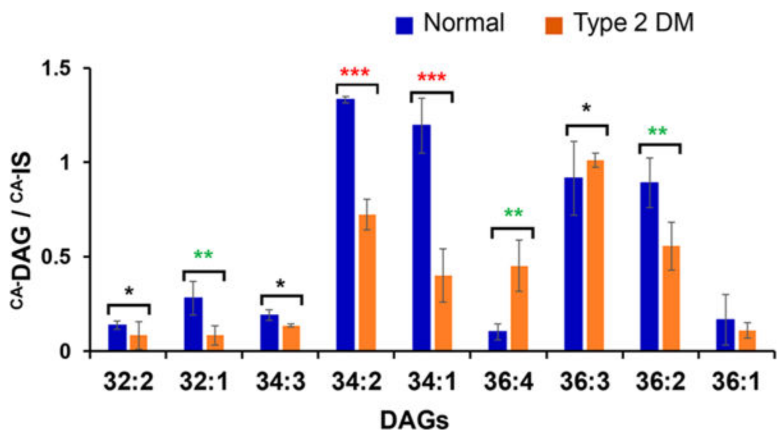

Figure 5.

Comparison of relative amount of major unsaturated DAGs in human plasma samples from normal control and type 2 DM patient. One μM of the internal standard (DAG 15:0/18:1-d_7/0:0) was added before the derivatization step. Error bars represent standard deviation; n = 3, *p < 0.05, **p < 0.01, ***p < 0.001 (t test).

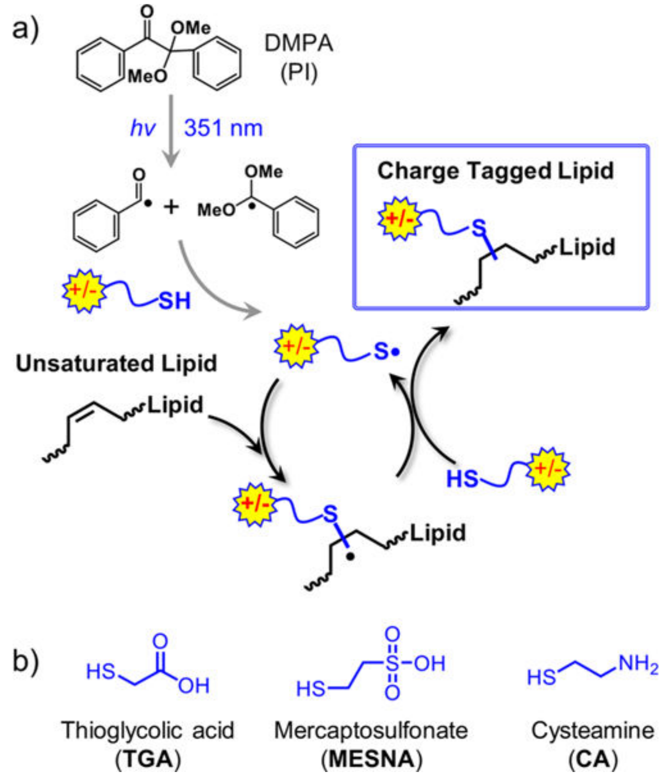

Scheme 1. (a) Charge Tagging of Unsaturated Lipid via Thiol–ene Click Chemistry[a] and (b) Chemical Structures of the Three Thiol Reagents

[a]DMPA is a commonly used photoinitiator (PI) for thiyl radical formation upon 351 nm wavelength UV irradiation

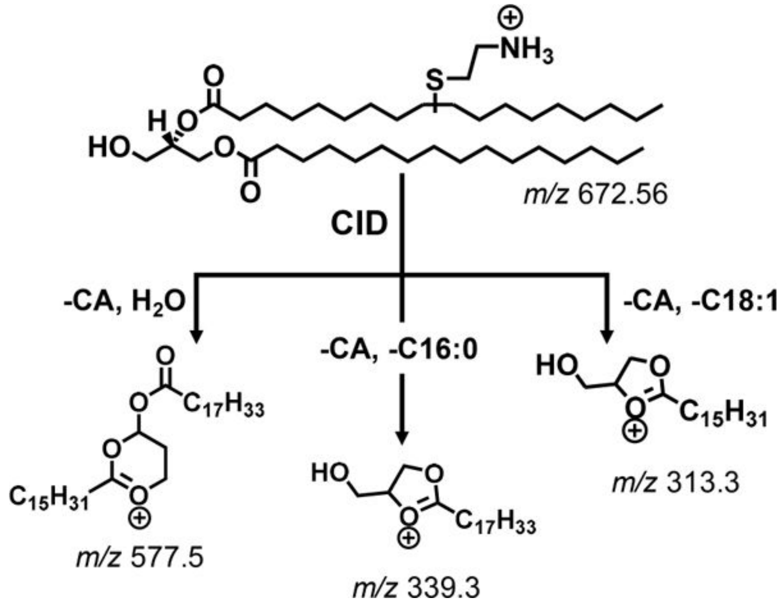

Scheme 2.

Proposed Structures for Fragments at *m/z* 577, 339, and 313 Resulting from CID of [$^{CA-}$DAG 16:0/18:1/0:0 + H]$^+$

Table 1

Identified DAG Species in Pooled Human Plasma

DAG	MW_(Da)	detection (*m/z*)	acyl chain composition	conc. (μM)
30:1	538.5	616.4	14:0_16:1	0.1 ± 0.01
30:2	536.5	614.3	14:1_16:1	0.08 ± 0.01
32:1	566.5	644.5	16:0_16:1/14:0_18:1	1.1 ± 0.1
32:2	564.5	642.5	16:1_16:1/14:0_18:2	0.7 ± 0.2
34:1	594.5	672.5	16:0_18:1/16:1_18:0	6.4 ± 1.0
34:2	592.5	670.6	16:0_18:2/16:1_18:1	7.7 ± 1.1
34:3	590.5	668.6	16:1_18:2/16:0_18:3	1.4 ± 0.3
36:1	622.5	700.4	18:0_18:1	1.3 ± 0.4
36:2	620.5	698.3	18:1_18:1/18:0_18:2	5.3 ± 0.6
36:3	618.5	696.3	18:1_18:2	6.0 ± 1.0
36:4	616.5	694.3	18:2_18:2/18:1_18:3	1.6 ± 0.6